THE JOURNAL OF BIOLOGICAL CHEMISTRY
Vol. 279, No. 16, Issue of April 16, pp. 16697–16705, 2004

Printed in U.S.A.

Oxidative Folding of *Amaranthus* α-Amylase Inhibitor

DISULFIDE BOND FORMATION AND CONFORMATIONAL FOLDING*

Received for publication, November 11, 2003, and in revised form, January 8, 2004
Published, JBC Papers in Press, January 28, 2004, DOI 10.1074/jbc.M312328200

Maša Čemažar‡§, Sotir Zahariev‡, Sándor Pongor‡, and Peter J. Hore¶

From the ‡International Centre for Genetic Engineering and Biotechnology, Padriciano 99, 34012 Trieste, Italy and the ¶Physical and Theoretical Chemistry Laboratory and Oxford Centre for Molecular Sciences, Oxford University, Oxford OX1 3QZ, United Kingdom

Oxidative folding is the fusion of native disulfide bond formation with conformational folding. This complex process is guided by two types of interactions: first, covalent interactions between cysteine residues, which transform into native disulfide bridges, and second, non-covalent interactions giving rise to secondary and tertiary protein structure. The aim of this work is to understand both types of interactions in the oxidative folding of *Amaranthus* α-amylase inhibitor (AAI) by providing information both at the level of individual disulfide species and at the level of amino acid residue conformation. The cystine-knot disulfides of AAI protein are stabilized in an interdependent manner, and the oxidative folding is characterized by a high heterogeneity of one-, two-, and three-disulfide intermediates. The formation of the most abundant species, the main folding intermediate, is favored over other species even in the absence of non-covalent sequential preferences. Time-resolved NMR and photochemically induced dynamic nuclear polarization spectroscopies were used to follow the oxidative folding at the level of amino acid residue conformation. Because this is the first time that a complete oxidative folding process has been monitored with these two techniques, their results were compared with those obtained at the level of an individual disulfide species. The techniques proved to be valuable for the study of conformational developments and aromatic accessibility changes along oxidative folding pathways. A detailed picture of the oxidative folding of AAI provides a model study that combines different biochemical and biophysical techniques for a fuller understanding of a complex process.

Cracking the code for folding a string of amino acid residues into a biologically active three-dimensional structure is still a major challenge of both chemical and biological interest. The information that determines the folding of a protein is contained solely in its amino acid residues (1). In proteins that contain cysteine residues the formation of disulfide bonds is an additional degree of freedom in the folding process. In these proteins a fusion between the recovery of the native tertiary structure (conformational folding) and the regeneration of native disulfide bonds is coupled in the oxidative folding process (2).

Disulfide formation is important for *in vivo* folding of a considerable number of eukaryotic proteins and is a key post-translational modification for the stabilization of folded structures. The study of oxidative folding *in vitro* can provide a detailed structural description in terms of the disulfide intermediate species present along the pathway of the complex folding process. A thorough account of an oxidative folding reaction should combine a study of the formation of covalently stable intermediate species and their disulfide bond connectivity and an analysis of the conformational assembly of these species. An established method for elucidation of the exact role that disulfides play in the process of achieving the native fold is time-resolved RP-HPLC[1] analysis of acid-trapped samples from an oxidative folding reaction. On the other hand, conformational folding is followed by physicochemical, mostly spectroscopic techniques, which give information at the level of a single residue or even a single atom in the polypeptide structure and are hence most versatile for looking at the restoration of native secondary and tertiary structures.

The regeneration of native disulfide bonds of several disulfide-rich proteins has been characterized showing a complex diversity of folding pathways that regulate native disulfide bond formation. The original studies on bovine pancreatic trypsin inhibitor by Creighton (3) were later revisited by Weissman and Kim (4), which resulted in one of the most extensively studied oxidative folding pathways and a major protein-folding model. Various aspects of disulfide formation, folding, and unfolding have also been studied for ribonuclease A (RNase A) (2, 5–8), which has become another well understood model system. Chang and co-workers (9–18) have studied extensively the oxidative folding mechanisms of various three- and four-disulfide proteins and have found different mechanisms, which reflect the variety of ways in which the native disulfide bonds in a protein are stabilized. Hirudin (11, 12), tick anticoagulant protein (18), and potato carboxypeptidase inhibitor (10, 14) share a common mechanism with a high heterogeneity of one-, two-, and three-disulfide intermediates, some of which have non-native disulfides. Epidermal growth factor (EGF) (13) forms both non-native three-disulfide isomers as well as a predominant species with two native disulfides (EGF-II). There are other proteins with predominant oxidative folding interme-

* This work was supported in part by the Engineering and Physical Sciences Research Council and by the Medical Research Council through the Oxford Centre for Molecular Sciences. The costs of publication of this article were defrayed in part by the payment of page charges. This article must therefore be hereby marked "*advertisement*" in accordance with 18 U.S.C. Section 1734 solely to indicate this fact.

§ Recipient of an International Centre for Genetic Engineering and Biotechnology predoctoral fellowship. To whom correspondence should be addressed. Tel.: 39-040-3757340; Fax: 39-040-226555; E-mail: cemazar@icgeb.org.

[1] The abbreviations used are: RP-HPLC, reverse-phase high performance liquid chromatography; EGF, epidermal growth factor; EETI-II, *Ecballium elaterium* inhibitor-II; photo-CIDNP, photochemically induced dynamic nuclear polarization; AAI, *Amaranthus* α-amylase inhibitor; MFI, main folding intermediate; Fmoc, *N*-(9-fluorenyl)methoxycarbonyl; GdnHCl, guanidine hydrochloride; DTT, dithiothreitol; FMN, flavin mononucleotide; 1D, one-dimensional; R, reduced (species); N, native (species).

diates that are only partially oxidized and contain only native disulfide bonds, for example hen egg white lysozyme (19), trypsin-specific squash inhibitor from *Ecballium elaterium* (EETI-II) (20), the cyclotide kalata B1 (21), and insulin-like growth factor-I (22). In contrast to the formation and reshuffling of disulfides commonly studied using acid trapping and RP-HPLC, the change in conformation at the level of amino acid residues, along the folding pathway, is poorly understood. The only study to have yielded kinetic data from an NMR experiment shows how to extract time constants for the development of native chemical shifts in hen egg white lysozyme (23). On the other hand the structures of several oxidative folding intermediates and their variants have been partially or fully elucidated with NMR (19, 24–33), x-ray crystallography (29), circular dichroism (34–37), fluorescence, Fourier transform infrared, and, in one case, also photo-CIDNP (25).

The oxidative folding of a cystine-knot three-disulfide-bonded protein, *Amaranthus* α-amylase inhibitor (AAI) (33, 38–42), is investigated in the present work. The cystine-knot motif is known for the high structural stabilization of its protein scaffold that makes it suitable for molecular engineering and drug design (43). The oxidative folding of AAI has been characterized (33) to include many heterogeneous disulfide intermediate species along its folding pathway, and their disulfide structures have been determined. Apart from the native species (disulfide bonds: 1–18, 8–23, and 17–31), five other three-disulfide species appear on the folding pathway, all of which contain non-native disulfide bonds (see Fig. 1*A*). Most interestingly, three of them also include the vicinal disulfide bridge between adjacent cysteine residues 17 and 18, one of which is the most abundant intermediate (MFI) of the folding process. These intermediates (MFI, I-5, and I-6) appear to be the first folding intermediates observed to have a vicinal disulfide bond. MFI has been studied in detail for its tertiary structure and the solvent accessibility of aromatic residues Tyr^{21}, Tyr^{27}, Tyr^{28}, and Trp^{5} (33). Because of its "bead-like" disulfide structure (1–8, 17–18, 23–31) and the high contact order that it confers, MFI has been assigned a significant role in the folding process (33).

The present work examines the kinetic process of oxidative folding of AAI at the level of individual disulfide species and at the level of individual amino acid residues. Firstly, the acid-trapping technique and RP-HPLC were combined to understand the stabilization of cystine-knot disulfides and the kinetics of their formation in different folding conditions. It was found that the cystine-knot disulfide bonds are interdependent and form via several kinetic traps, of which MFI is favored due to its statistically probable disulfide pattern. Secondly, spectroscopic techniques (NMR and photo-CIDNP) were used to give information about the conformational characteristics of the disulfide species present on the folding pathway. The tertiary structure and solvent accessibility of aromatic residues were examined in a time-resolved experiment for the entire oxidative folding process and contrasted to the equilibrium species that are a part of the folding assembly at any time during the refolding process. This is the first oxidative folding process to be elucidated in a time-resolved manner using 1D NMR and photo-CIDNP. The rate constant of formation of the native AAI protein was found to be the same at the disulfide species and single residue levels.

EXPERIMENTAL PROCEDURES

Peptide Synthesis

AAI peptide was produced manually on a 1-mmol scale by solid-phase peptide synthesis using an Fmoc (*N*-(9-fluorenyl)methoxycarbonyl) methodology (33, 39). The crude peptide was isolated with yield >90% and purified to homogeneity (>98%, RP-HPLC). The procedure was essentially as described elsewhere (39), with the exception of cysteine residues, which were introduced as Fmoc-Cys(Trt)-OPfp (33, 44).

Reverse-phase HPLC and Electrospray Ionization-Mass Spectrometry

Analytical and preparative reverse-phase HPLC were carried out on a GILSON® system, configured with an 805 manometric module, an 811 C dynamic mixer with two model 306 pumps and a model 118 UV-visible detector, computer-controlled GILSON® 506 C system module, and Unipoint system software. Analytical separation was done on a ZORBAX 300 SB-5C18 (150 × 4.6 mm, inner diameter, Hewlett Packard) column at flow rates of 0.8 or 1.0 ml min^{-1}. Preparative RP-HPLC was done on a Waters Prep LC Universal base module with a Prep-Pac® cartridge Delta Pac 300 15RC18 (100 × 40 mm, inner diameter, Waters) column at a flow rate of 15 ml min^{-1}. Samples were eluted with linear gradients of solvents A (H_2O, 0.1% trifluoroacetic acid) and B (CH_3CN, 0.1% trifluoroacetic acid). The disulfide connectivities of intermediates were determined as described elsewhere (33). The detailed conditions of oxidative folding from native AAI and MFI, reductive unfolding from native AAI and MFI, and folding in the presence of guanidine hydrochloride (GdnHCl) and DsbC are all indicated in the corresponding figure legends. The presence of disulfide species at different times after the start of folding was examined by removing aliquots from the folding mixture at selected time points and analyzing them with analytic RP-HPLC. The pH of oxidative folding reaction in the presence of DsbC was chosen to be 7.40 to approximate it to physiological conditions. Electrospray ionization-mass spectrometry experiments were performed on a PerkinElmer Life Sciences API 150 EX electrospray, single quadrupole mass spectrometer operated at a resolution of 3000. The samples were analyzed in positive mode either by direct syringe infusion or via a liquid chromatography-mass spectrometry system using two Waters model 510 pumps and a microbore column (Agilent ZORBAX 300 SB-C18, 1.0 × 150 mm, 3.5 μm) and applying a gradient of 0–60% B (60 min) at a flow rate of 40 μl min^{-1}. The molecular weights of the peptides were calculated using the Applied Biosystems software (BioMultiview and ProMac).

NMR and Photo-CIDNP Spectroscopy

Sample Preparation—Samples for equilibrium spectra of native, MFI, and reduced AAI were purified by analytic RP-HPLC at pH 2, lyophilized, and redissolved in D_2O at pH 7 immediately prior to experiment. Samples for time-resolved spectra were obtained by refolding reduced AAI (6SH) ([AAI] = 50 mg/liter, 0.1 M NH_4OAc, 2 mM EDTA, 1.0 M GdnHCl, pH 8.5, 1 mM cysteine, 0.05 mM cystine, 25 °C) and acid quenching (with trifluoroacetic acid to pH 2) of 10.0-ml aliquots at various refolding times. The protein content was separated from the refolding buffer with RP-HPLC (gradient of 0–60% B in 10 min). Samples were lyophilized and kept under N_2 at 4 °C before they were redissolved in D_2O (pH 7), and 0.2 mM flavin mononucleotide (FMN) was added for photo-CIDNP experiments. The stability of the samples was confirmed by comparing analytical RP-HPLC profiles before lyophilization (after purification) and after the NMR/photo-CIDNP experiment.

Spectra Acquisition—All NMR spectra were recorded on home-built 600 NMR spectrometers (Oxford Centre for Molecular Sciences) with operating frequencies of 600.20 MHz. The spectrometers are equipped with Oxford Instruments Co. magnets, Omega software, digital control equipment (Bruker Instruments), home-built triple resonance probe heads, and home-built linear amplifiers (45). For photo-CIDNP experiments, the light of a 4-watt continuous wave argon ion laser (Spectra-Physics Stabilite 2016-05) with 100-ms light pulses was introduced into the NMR tube via an optical fiber (diameter 1 mm), inside a coaxial Pyrex insert (Wilmad WGS 5BL) (46). Spectra were recorded at 25 °C and pH 7. Both NMR and photo-CIDNP spectra were recorded with 10,000 Hz spectral width, 4096 block size, and 512 and 16 acquisitions, respectively. All NMR data were processed using Felix 2.3 software from Biosym Technologies.

RESULTS

Oxidative Folding at the Level of Disulfide Species

The oxidative folding process of AAI was first studied at the level of individual disulfide species. The intermediate species, which take part in the folding process, were all characterized previously in terms of their disulfide content, which is shown as a summary in Fig. 1*A* (33). They are all covalently bonded stable species, which are efficiently separated with analytic RP-HPLC at acidic pH (4). A time-resolved analysis of their

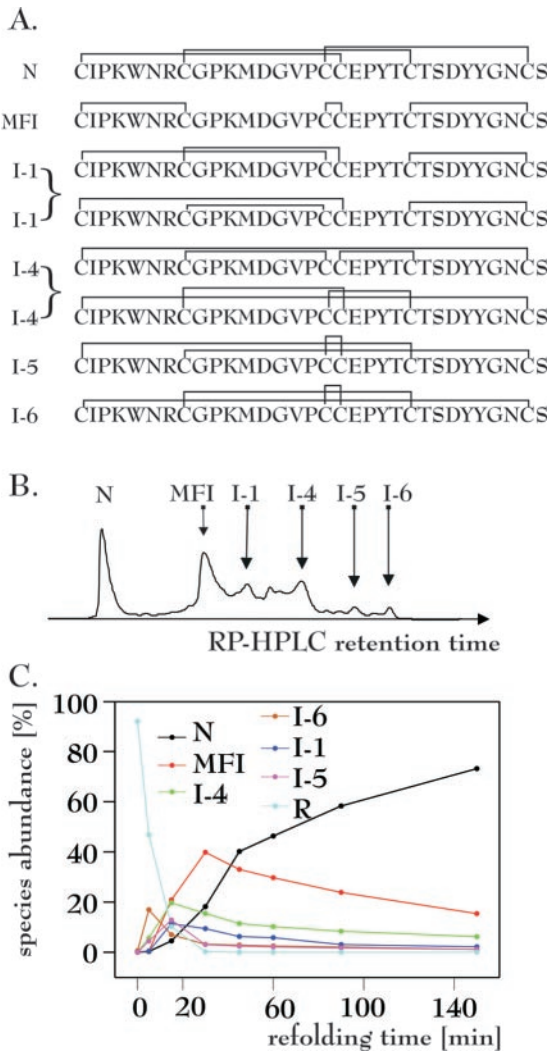

FIG. 1. *A*, disulfide bonds in the observed three-disulfide species: a summary and a comparison of all disulfide bonds that appear in three-disulfide species of AAI protein. Apart from the native protein, which was confirmed to have the *abc abc* topology, the prevailing disulfide bond appearing in three different species is the vicinal linkage Cys^{17}-Cys^{18}. For I-1 and I-4, the two possible arrangements are shown. *B*, RP-HPLC profile of the separation of the oxidative folding mixture in the optimum conditions after 45 min of refolding with a gradient of 0–20% B (5 min) followed by 20–27% B (30 min), at a flow rate of 0.8 ml min^{-1}. The elution positions of all three-disulfide species are shown. *C*, the abundances of all fully oxidized species and the fully reduced protein are plotted *versus* the refolding time. Their abundances are taken from the intensities of the RP-HPLC peaks and are calculated from their absorbance at 214 nm.

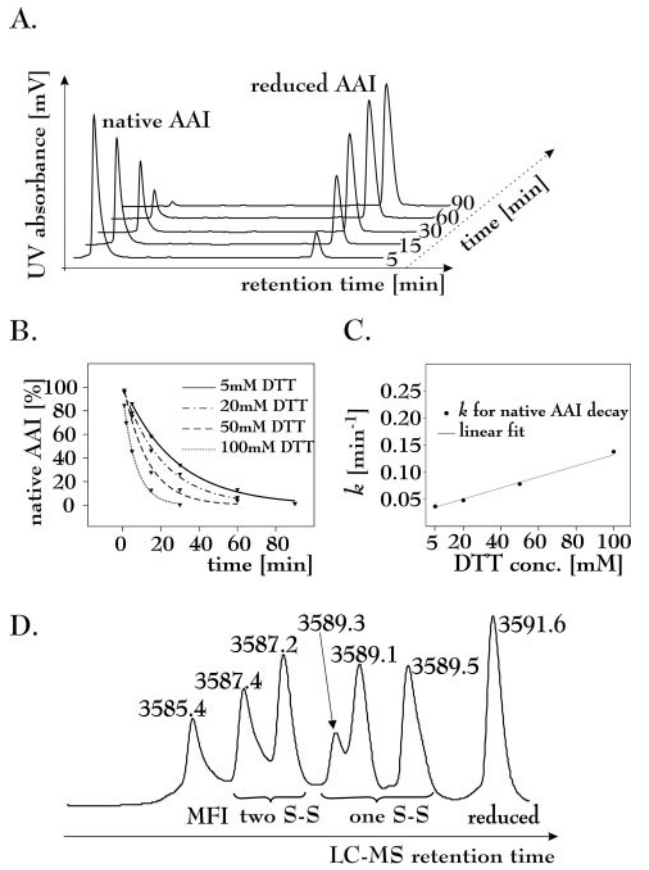

FIG. 2. *A*, time-resolved RP-HPLC profiles for reduction of native AAI with 5 mM DTT at different times after initiation. The reverse process of oxidative folding starts from purified native AAI species, which, in the presence of a reducing agent, unfolds and gets reduced to form the fully reduced state (conditions: 0.5 mg/ml AAI, 0.1 M NH_4OAc, pH 8.50, 25 °C). *B*, native AAI decay at different concentrations of DTT (5, 20, 50, or 100 mM); abundance of native AAI is plotted against reduction time. The decay is fitted to a first order exponential decay curve for each DTT concentration. *C*, the rate constants for native AAI decay (extracted from *B*) plotted *versus* DTT concentration (*conc.*) and fitted to a straight line. *D*, reductive unfolding of MFI (0.5 mg/ml MFI, 0.1 M NH_4OAc, pH 3.0, 100 mM Tris(2-carboxyethyl)phosphine, 25 °C) examined by liquid chromatography-mass spectrometry (*LC-MS*). The profile shows the mixture of products after 2-min reduction. The molecular masses of each species are shown, which determine their disulfide content. A reverse-phase C_{18} analytic column (5 μm) and a gradient of 0–20% B (5 min) followed by 20–30% B (30 min) at a flow rate of 0.8 ml min^{-1} were used.

transformations was performed in different folding conditions.

Heterogeneous Mixture of Intermediates in the Optimum Oxidative Folding Conditions—The first experiment was the refolding of reduced AAI at the optimum oxidative folding conditions, which have been described before (33), where over 93% of the native protein is regenerated in 20 h. The chromatogram, which shows the separation of the reaction mixture 45 min after the start of the reaction, is shown in Fig. 1*B*. The optimized oxidative folding of AAI is characterized by a high heterogeneity of one-, two-, and three-disulfide species. It is dominated by only a few disulfide species, among which are especially prominent the five fully oxidized species with three disulfide bonds (MFI, I-1, I-4, I-5, and I-6). A plot of the abundance of all three-disulfide species and of the fully reduced protein *versus* the refolding time is shown in Fig. 1*C*. The rapid disappearance of the reduced species is fitted well to a first order exponential decay ($R^2 > 0.99$, where R is the multiple correlation coefficient) with a rate constant of 0.14 min^{-1}. The native species accumulates with a lower rate constant, and the data for the first 20 h of folding is fitted well to a first order exponential rise curve, where 0.0098 min^{-1} is the rate constant ($R^2 > 0.99$). The sigmoidal build-up of the signal during the first 30 min (Fig. 1*C*) has a negligible effect on the quality of the fitting.

Interdependence of Disulfides in Native AAI and Their Independence in the MFI Species—The mechanisms of reductive unfolding of native AAI protein and the main folding intermediate species were analyzed to give information about the way these two different disulfide patterns are stabilized. Purified native AAI protein was isolated and placed into a reducing buffer containing various concentrations of dithiothreitol (DTT) at pH 8.50. The unfolding experiments were quenched in a time course manner and analyzed by RP-HPLC. The results show that the reduction of the native species leads to direct conversion to the fully reduced species, without accumulation of intermediate one-, two-, or three-disulfide species (Fig. 2*A*).

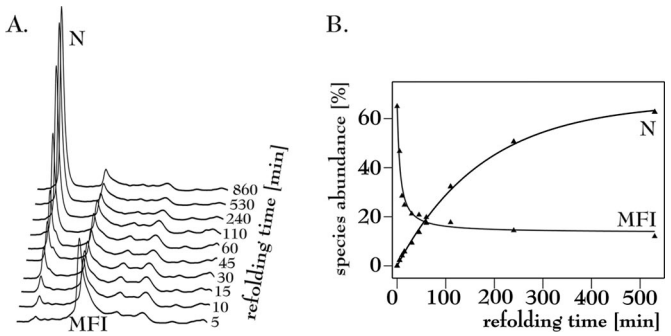

FIG. 3. *A*, oxidative folding starting from purified MFI species (100 mg/liter MFI, 0.1 M NH_4OAc, 2 mM EDTA, 1.0 M GdnHCl, pH 8.50, 1 mM cysteine, 0.05 mM cystine, 25 °C). Time-resolved RP-HPLC chromatograms show the separation of folding mixtures at different times after the start of oxidative folding. *B*, the abundances of native AAI and MFI species (from data in *A*) are plotted *versus* refolding time and fitted to first order exponential curves.

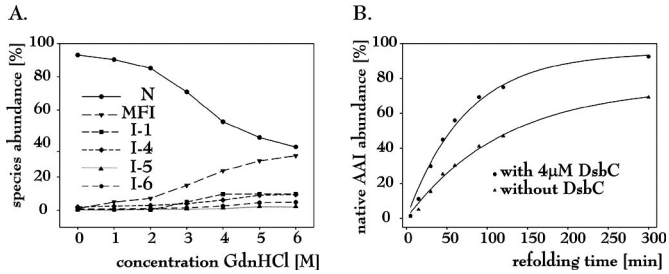

FIG. 4. *A*, oxidative folding in the presence of guanidine hydrochloride; the abundances of three-disulfide species were extracted from the time-resolved RP-HPLC chromatograms of folding mixtures after 24 h of oxidative folding and plotted *versus* the concentration of GdnHCl. The oxidative folding conditions were kept constant (100 mg/liter AAI, 0.1 M NH_4OAc, 2 mM EDTA, 1.0 M GdnHCl, pH 8.25, 1 mM cysteine, 0.05 mM cystine, 25 °C), while GdnHCl concentration is varied from 0 to 6.0 M. *B*, DsbC-assisted oxidative folding; the abundances of native AAI species were extracted from the time-resolved RP-HPLC chromatograms of folding mixtures and plotted *versus* the refolding time. The oxidative folding conditions were kept constant (100 mg/liter AAI, 0.1 M NH_4OAc, 2 mM EDTA, 1.0 M GdnHCl, pH 7.40, 1 mM cysteine, 0.05 mM cystine, 25 °C), while 4 μM DsbC was either present or absent. Comparison of formation of native AAI with and without DsbC at the same conditions was evaluated by calculating the abundance from absorbance detected at 214 nm. Both sets of data are fitted to a first order exponential growth curve.

This concurrent reduction is observed for different concentrations of the reducing agent, ranging from 5 to 100 mM. The rate constant for the conversion of the native AAI to the reduced species ($k_{N\rightarrow R}$), extracted for four different DTT concentrations (Fig. 2*B*), shows a linear dependence upon the concentration of DTT, as seen in Fig. 2*C*. The unfolding pathway was also examined with Tris(2-carboxyethyl)phosphine as a reducing agent (pH 3.0) and was found to be mechanistically unchanged.

In contrast to the reductive unfolding of the native species, the mechanism of the same process for MFI, studied by liquid chromatography-mass spectrometry, turned out to be very different. A sample profile, showing the mixture of products after 2-min reduction of purified MFI, is shown in Fig. 2*D*. MFI forms two two-disulfide isomers and three one-disulfide isomers as intermediates during reductive unfolding. The retention times of these isomers do not coincide with those of any other species on the oxidative folding pathway from reduced AAI, so they probably contain only MFI–disulfide bonds and are formed when each MFI-disulfide is reduced in turn.

Oxidative Folding from MFI—The folding pathway from the purified MFI species was studied to examine the kinetic role of MFI in the oxidative folding pathway of AAI protein. It was purified from the refolding mixture obtained 30 min after the start of folding from reduced protein, when it is present at ~40% abundance. It was then re-inserted into the oxidative folding buffer. The chromatograms obtained at different times of folding are shown in the Fig. 3*A*. The rate constant for formation of native AAI is 0.0057 min^{-1} (Fig. 3*B*), which is about half that found for folding from the reduced AAI protein under the same conditions (0.0098 min^{-1}). A very similar folding pathway to the one proceeding from reduced AAI is observed in terms of the presence of the disulfide species formed. All three-disulfide intermediates (I-1, I-4, I-5, and I-6) accumulate to significant amounts. The reduced state was not detected.

MFI Prevails in the Absence of Secondary and Tertiary Interactions—The fully reduced AAI protein was refolded in the presence of different concentrations of GdnHCl, which was used to disrupt the native structural preferences and interactions. We were interested to examine how the formation of native disulfides is influenced by partially or completely removing such preferences and interactions. The refolding reaction was monitored by time-resolved RP-HPLC. The chromatograms obtained from the folding mixtures 24 h after the initiation of the folding reaction, containing from 0 to 6.0 M GdnHCl, were analyzed, and the abundances of the three-disulfide species were plotted against GdnHCl concentration (Fig. 4*A*). The reactions in the absence of GdnHCl and in its presence at 1.0 M concentration yield very similar results, reaching over 90% of native AAI product. As the concentration of GdnHCl is gradually increased to 6.0 M, the amount of native species obtained after 24 h of refolding decreases rapidly, and native AAI represents only 38% of all protein conformations at 6.0 M GdnHCl. At the same time, the other three-disulfide species (MFI, I-1, I-4, I-5, and I-6) are becoming more abundant, especially MFI, which reaches 32% at 6.0 M GdnHCl. This species is clearly favored over the other three-disulfide species, whose individual abundances never reach more than 10%.

Mimicking Oxidative Folding in Vivo—To examine oxidative folding in conditions similar to those in the endoplasmic reticulum, AAI was refolded in the presence of disulfide isomerase enzyme DsbC and studied by RP-HPLC. All three-disulfide species observed previously under optimum refolding conditions (MFI, I-1, I-4, I-5, and I-6) are present on this pathway. However, MFI is not the most abundant intermediate species; this is now I-1. The kinetics of native AAI formation was examined and compared with measurements under the same conditions in the absence of DsbC, seen in Fig. 4*B*. Both kinetics fit well to a first order exponential growth curve ($R^2 > 0.99$) and have the following rate constants for the formation of native AAI protein: 0.014 min^{-1} with DsbC and 0.0083 min^{-1} without DsbC. The final yield of native AAI under these conditions is larger when the folding is assisted by DsbC (94% *versus* 75% in the absence of DsbC). It has to be noted, however, that the high yield of formation of native AAI peptide in the presence of DsbC (94%) is comparable with that obtained in the optimum refolding conditions (93%), described above. The rate constant of formation of native AAI is increased from 0.0098 min^{-1} in optimum refolding conditions to 0.014 min^{-1} in the presence of DsbC.

Oxidative Folding at the Level of Individual Residues

To follow the conformational changes that accompany the formation of native disulfide bonds at the level of individual amino acid residues, a series of experiments using 1D ^1H NMR and photo-CIDNP spectroscopy was carried out. As in the studies described above, the properties of the known equilibrium species appearing on the folding pathway were elucidated. Using both NMR and photo-CIDNP, the 1D spectra of the three most abundant species of the oxidative folding reaction (native

AAI, MFI, and reduced AAI) were compared with the time-resolved spectra obtained from the folding mixture.

Time-resolved NMR Study—The tertiary folds of the three milestones of the folding pathway of AAI were first elucidated with equilibrium NMR. Purified reduced (R), MFI, and native (N) samples were used to obtain orientation spectra for the conformational arrangements along the folding pathway (Fig. 5, *A* and *B*, *right hand*). Chemical shift assignments of the native state were taken from Lu *et al.* (40); assignments for the aromatic region as well as some assignments in the aliphatic region of MFI were obtained previously from 1D photo-CIDNP and two-dimensional COSY experiments (33). Some reduced species assignments were obtained from 1D photo-CIDNP. The spectra of R show a series of fairly well resolved lines corresponding to the resonances of the component amino acid residues in similar environments. However, this species does not display a completely random coil conformation. The corresponding spectra of the N state include significant dispersion in chemical shifts, a typical characteristic of native tertiary folds with persistent tertiary features. The NMR spectrum of the purified MFI species resembles that of the N state; the chemical shifts are well dispersed and the lines narrow, but MFI shows additional weaker signals, owing to minor conformation(s) present aside from the main conformation (33). The equilibrium spectra of these three species were compared with the time-resolved spectra to look for the characteristics of the conformational folding assembly at different times of the refolding reaction. For the time-resolved experiments the protein species were separated from the refolding buffer using RP-HPLC, which also made the aliquots more stable while acquiring the NMR data. The NMR experiments were done on aliquots of protein assemblies from the folding reaction, which were stopped at different times after initiation.

The aromatic region of the NMR spectra is shown in Fig. 5*A*. Here the NMR signals of four aromatic residues (Tyr^{21}, Tyr^{27}, Tyr^{28}, and Trp^{5}) are shown for the equilibrium species and the time-resolved samples. There are several examples of how a peak with a native chemical shift develops through the folding reaction, for example Tyr^{27}(H2,H6) and Trp^{5}(H7), which are distinguishable already after 45 and 90 min of the folding reaction, respectively. The peaks belonging to MFI appear almost immediately after the start of the reaction (15 min) and slowly, but not completely, disappear from the folding assembly. Even after 1200 min, there is some MFI present in the mixture; the best resolved example of an MFI peak is TyrC(H3,H5).

The time-resolved spectra of the aliphatic region of the ^{1}H NMR (Fig. 5*B*) show a similar picture, although there are fewer lines as well resolved and as representative of the three equilibrium species. Three native resonances are partially restored as early as 45 min after the initiation of the folding reaction: Thr^{22}(Hγ2), Val^{15}(Hγ1), and Val^{15}(Hγ2). The chemical shifts of the signals for MFI and the reduced species in this region are almost entirely overlapping, so one cannot say much with certainty about the disappearance of the reduced state and the appearance of MFI. The only peak which is distinguishably non-native is Thr^{22}(Hγ2), but even here MFI and R signals overlap.

Time-resolved Photo-CIDNP Study—Photo-CIDNP is a powerful tool for the elucidation of residue-specific surface accessibilities of aromatic side chains that uses a laser-initiated, reversible photochemical reaction between the protein and a flavin photosensitizer dye (FMN) to generate nuclear spin polarizations that result in enhancements in the intensities of the corresponding NMR signals. Photo-CIDNP experiments monitor not only the restoration of the native state and the abundance of various intermediates at different times but also the accessibility of the four aromatic residues during the oxidative folding process. In this experiment the NMR signal intensity can be diminished by several factors but primarily by the presence of the cysteine thiol groups.

First, preliminary experiments were done on all principal components of the folding buffer to test them for quenching effects on the FMN sensitizer polarization. Cysteine, which is present at 1.0 mM concentration, was found to have a strong quenching effect on the triplet state of FMN, which is responsible for the formation of radical pairs and the consequent signal enhancement of the aromatic side chains of amino acid residues (47). This quenching phenomenon was assigned to its thiol group, well known to quench the FMN triplet state without production of CIDNP (48). The oxidative folding buffer contains several other components at reasonably high concentrations (*i.e.* 0.1 M NH_4OAc, 1.0 M GdnHCl) with respect to those of the protein and the photosensitizer dye. For this reason non-protein components of the refolding buffer were removed as described under "Experimental Procedures." In the equilibrium photo-CIDNP spectra (*right hand* of Fig. 5*C*) of the three milestone species, all four aromatic residues (Tyr^{21}, Tyr^{27}, Tyr^{28}, and Trp^{5}) contribute. In the photo-CIDNP spectrum of the N species Tyr^{27} and Tyr^{28} are clearly accessible, but Tyr^{21}, which has a much weaker enhancement, seems less so. MFI shows accessibility for all three tyrosine residues, both in its major and minor conformations. The spectrum of the reduced species is similar to that of MFI, and although this spectrum has not been assigned entirely, we can expect that the signals observed come from all four aromatic side chains. The signal intensity of this spectrum is somewhat reduced by the presence of the six thiol groups.

The time-resolved photo-CIDNP spectra can again be analyzed in terms of the native, MFI, and reduced spectra. The reduced peaks disappear within 30 min of the initiation of the folding reaction, and this is especially clear for the Trp^{5}(H4) peak, which does not overlap with its native or MFI equivalents. Most of the MFI peaks overlap with the signals of both N and R. However, the emissive peaks of the (H3,H5) protons of TyrC and TyrA residues are well separated. They appear soon after the start of the folding and have significant abundance up to 150 min. The restoration of the native state is confirmed by the Trp^{5} and $Tyr^{27,28}$(H3,H5) resonances. It can be seen that from 45 min onward there is some accumulation of the native state, which prevails from about 120 min onward. Very similar time-resolved NMR and photo-CIDNP spectra were obtained at two different pH values: at pH 2 (data not shown), where disulfide exchange is minimized, and at pH 7, a more representative pH for physiological reactions *in vivo*.

Comparison between Individual Species and Individual Residue Studies—It is important that the results obtained using these techniques are examined for their credibility. Fig. 6 shows the kinetics of formation of AAI obtained in different ways under the same conditions; all the rate constants are of the same order. The RP-HPLC study gave a rate constant of 0.010 min^{-1}, the aromatic NMR data 0.0080 min^{-1}, and the aliphatic NMR data 0.0064 min^{-1}. This indicates that time-resolved NMR experiments of this kind are a valuable technique for the study of conformational developments on an oxidative folding pathway.

DISCUSSION

The kinetics of oxidative folding has been studied at the levels of individual disulfide species and of individual residues within them. At the level of the various disulfide species, the kinetics in different conditions and the rate constants of formation of native AAI have been compared. The general mech-

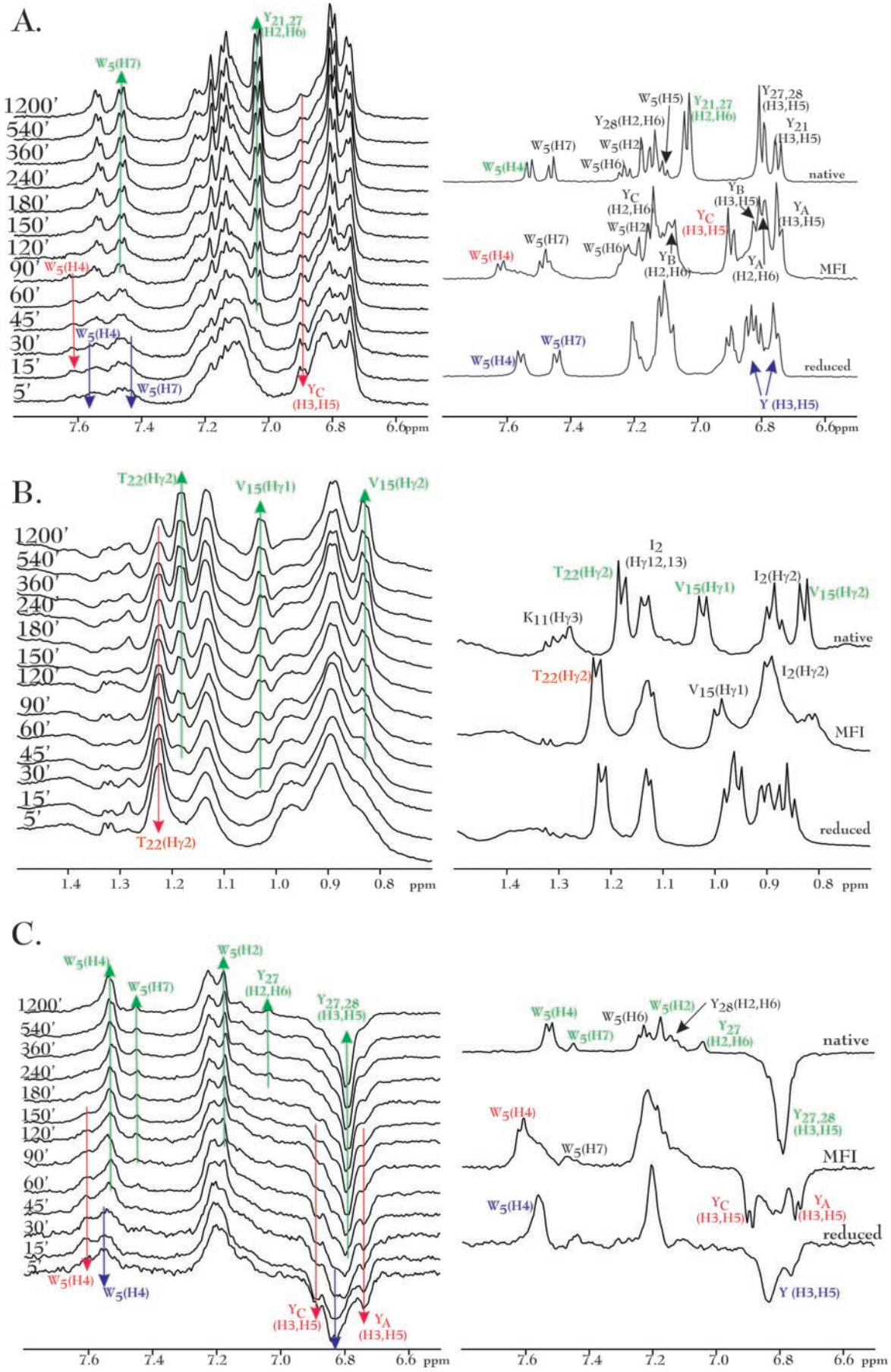

FIG. 5. *A*, *B*, and *C*, the *right hand* of the panels shows the equilibrium spectra of purified native AAI, MFI species, and reduced AAI. The *left-hand* spectra are time-resolved spectra of the oxidative folding mixtures at the times indicated on the *left margin*. Spectra were recorded at

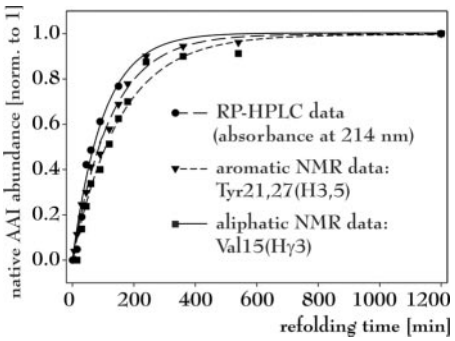

FIG. 6. **Comparison of NMR and HPLC study: the data for the formation of native AAI species are compared for the NMR and RP-HPLC study.** The data are extracted from absorbance at 214 nm in the RP-HPLC experiment. The data for the NMR experiment are extracted from the NMR signal intensities of the denoted peaks. Rate constants are calculated from the first order exponential curves, which are fitted to the data.

anism was found to be independent of the rate of formation of the native AAI protein, which depends on the conditions of the folding buffer. This has been observed previously for other oxidative folding pathways (16).

Combining the observations for oxidative folding and reductive unfolding, the kinetics of formation and stabilization of cystine-knot disulfides can be partially revealed. In the optimum folding conditions, the first non-native disulfide intermediate that accumulates is I-6, after which three other species (I-1, I-4, and I-5) emerge, followed finally by MFI, which reaches a maximum abundance of 40% 30 min after the start of oxidative folding. This means that the reshuffling and isomerization of the non-native disulfides in this intermediate are the slow, rate-determining step in the process.

The so-called "all-or-none" reductive unfolding mechanism observed for native AAI is shared by other small cystine-rich proteins, such as hirudin, potato carboxypeptidase inhibitor, and tick anticoagulant protein (9). The native disulfides of such proteins are stabilized in a concerted and interdependent manner because they do not allow for intermediate species when the native disulfide bonds are reduced. Another important observation is that these proteins, which share a common reductive unfolding mechanism, also have the same characteristics for the oxidative folding pathway. AAI and the above mentioned proteins all have a high heterogeneity of one-, two-, and three-disulfide species, including non-native disulfide isomers. On the other hand, the reductive unfolding from the three-disulfide species MFI with bead-like non-native disulfides shows the presence of one- and two-disulfide intermediates. This suggests that the disulfide bonds of MFI are not interdependent but are stabilized independently, probably because of the preference for forming disulfides between the cysteines that are closest to each other in the sequence.

Going back to oxidative folding, when MFI is isolated and re-inserted into the folding buffer its non-native disulfides have to be reduced and re-oxidized to reach the native state. The reductive unfolding of MFI suggests that its non-native disulfides are independent and therefore are likely to be reduced sequentially. This means that, for example, intermediates I-5 and I-6 can form from the one-disulfide species containing only the vicinal disulfide bridge (Cys^{17}-Cys^{18}), which is shared by MFI, I-5, and I-6. The fact that the reduced state was not detected could signify that MFI does not need to be completely reduced to start the folding process toward the native state. This is consistent with the independence of the disulfide bonds in MFI. It has been noted previously that fully oxidized intermediates involving non-native disulfides do not need to unfold and be reduced entirely for conversion to the native structure (11). MFI is, however, far from being an immediate precursor of the native state. The one- and two-disulfide species that form from MFI are either short lived, exist in a minute concentration, or their conversion to other three-disulfide species is spontaneous and irreversible (11). Even though the direct precursors of the native species are one- and two-disulfide species with native disulfides, the rate-determining step of folding will be their formation from the three-disulfide isomers, such as MFI, as suggested above. Species containing non-native disulfide bonds formed by oxidative folding that are stabilized by non-native tertiary interactions are kinetic traps. Such species are off-pathway intermediates, which have to overcome an energy barrier to unravel the structure they have already formed (16). MFI is in this sense an off-pathway intermediate in the oxidative folding from reduced AAI to the native state. It has to undergo a complex process of disulfide reshuffling from non-native to native bonds, during which it forms other fully oxidized species (I-1, I-4, I-5, and I-6).

In the presence of a high concentration of denaturant, which weakens the secondary and tertiary interactions that usually drive the folding process, MFI was the most abundant species apart from the native state. In the absence of a denaturant, secondary and tertiary preferences encoded in the amino acid sequence enable efficient conversion to the close packed native structure, which promotes the native disulfide pairing (1). At the same time, in small proteins such as AAI the native-like three-dimensional conformations are not unlikely to be able to accommodate non-native disulfide bonds and non-native disulfide topologies (33). On the other hand, it has been confirmed in recent years that even proteins under highly denaturing conditions with reduced disulfide bonds keep a non-random structural preference for the formation of secondary and tertiary structures (49). Also, hydrophobic interactions persist under strongly denaturing conditions (50), and compact molten globule structures can be present in the absence of disulfides (51). A similar phenomenon is observed as the concentration of denaturant is increased in the oxidative folding of AAI. The protein does not lose the preference of the primary sequence for the formation of the native structure with native disulfide bridges, which remains the most abundant species. Additionally, when some secondary and tertiary interactions are disrupted, the bead-like structure, in which disulfide bridges are formed from the cysteines nearest to each other within the sequence, has the highest probability of formation (12, 52). MFI is statistically the most probable disulfide conformation when reduced AAI protein is allowed to refold, and this is why its abundance increases as secondary and tertiary interactions are disrupted.

All the non-native three-disulfide species observed in the optimum refolding conditions were present on the pathway assisted by protein disulfide isomerase (DsbC), and of these MFI was not the most abundant. In an *in vitro* oxidative folding experiment the isomerization can be induced with a reducing agent, which is frequently a core part of the refolding buffer. In the case of AAI this role is taken up by cysteine, which keeps a high reducing potential to convert non-native disulfides into reactive thiols. *In vivo*, the reduction and isomerization of

1.0 mM AAI, 25 °C, pH 7.0, with 10,000 Hz spectral width, 4096 complex points. *A*, 600-MHz 1D ^{1}H NMR spectra of oxidative folding of AAI, aromatic region, 512 acquisitions. *B*, 600-MHz 1D ^{1}H NMR spectra of oxidative folding of AAI, aliphatic region, 512 acquisitions. *C*, 600-MHz 1D ^{1}H photo-CIDNP spectra of oxidative folding, aromatic region, 16 acquisitions, and 100-ms laser flashes. FMN was added at 0.2 mM concentration.

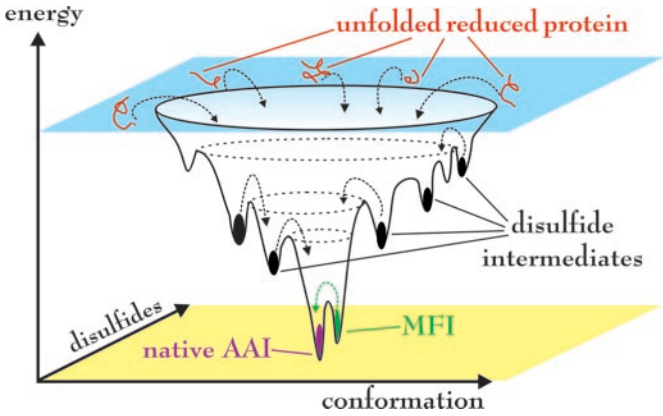

FIG. 7. **A schematic representation of the energy landscape of oxidative folding of AAI, designed by modifying a general protein-folding energy landscape (60).** The energy of the protein is displayed as a function of which disulfide bonds are present and the extent of conformational folding. The local minima represent non-native disulfide intermediates like MFI, which are kinetic traps.

non-native disulfides made early in the oxidative folding process are essential to avoid misfolding. This is mostly achieved with the help of a folding catalyst, for example protein disulfide isomerase, which catalyzes the rearrangements that lead to native disulfides and native tertiary structure (53). Disulfide isomerase proteins have been found previously in numerous other plant organisms, such as soybean (54), wheat (55, 56), maize (57), and rice (58). It is therefore highly probable that *Amaranthus* crop plants have a gene for a disulfide isomerase. To approximate the conditions of oxidative folding *in vivo*, the bacterial homologue DsbC was used, whose three-dimensional structure is known to contain two active sites for disulfide reduction and isomerization (59). AAI is a small protein relative to the DsbC molecule, which is a homodimer containing over 400 amino acid residues. The efficiency of reduction and isomerization of the non-native disulfides of AAI depends on their accessibility to the DsbC active sites. Although these active sites are well exposed on the surface of DsbC protein, it might not be easy to access the "hidden" disulfides of a cystine knot. Structures with more solvent-exposed disulfides are probably isomerized more efficiently. This last observation could be an explanation for the fact that MFI is not as abundant in the folding assisted by DsbC because a bead-like disulfide pattern probably has a high disulfide accessibility. The energy barrier for conversion of MFI to one- and two-disulfide species could be lowered in this way.

This is the first time that time-resolved NMR and photo-CIDNP studies have been used to analyze a complete oxidative folding pathway and the first time that the latter technique has been applied to this kind of process. Both techniques proved to be valuable for the study of conformational developments and aromatic accessibility changes along the oxidative folding pathways. The rate constants for native AAI formation compared favorably with the data from RP-HPLC studies. The results give a description at the level of individual residues of the formation of the native three-dimensional structure. Combining these results, which give information about the effect of non-covalent interactions that drive the search for the native conformation, with the information about the abundances and kinetics of interconversion of the different disulfide pairings, we get a more detailed picture of the oxidative folding. It has to be noted, however, that some intensity in the NMR peaks thought to belong to a specific species, for example MFI, could be partially contributed by other disulfide intermediates with similar structural features. Therefore, the NMR signals could be regarded as representative of a specific structural environment for the residue in question. Photo-CIDNP intensities cannot be used in quantitative comparisons of data because they do not reflect solely the abundances of different species.

An interesting observation concerns the number and intensities of the peaks in the region between 6.7 and 6.9 ppm of the time-resolved photo-CIDNP spectra. In this part of the AAI spectrum, the resonances belonging to Tyr(H3,H5) protons appear as emissive peaks. At the beginning of oxidative folding, there is a large number of resonances representing the large number of species and conformations in which Tyr(H3,H5) side chains are accessible. The intensities of some of these peaks gradually decrease, and eventually some disappear. As the folding proceeds, one principal signal grows in intensity (that belonging to native Tyr[27,28]). The disappearance of the other emissive peaks corresponds to the disappearance of the protein conformations in which the tyrosine side chains are accessible to the solvent. Indirectly, this could also be seen as the funneling of a large number of conformations toward a more compact, native tertiary scaffold with fewer accessible side chains.

If we try to imagine a three-dimensional energy landscape of oxidative folding, the energy of the protein will be a function of which disulfide bonds are present and the extent of conformational folding (Fig. 7). The protein molecules will have folded successfully when they reach the lowest energy point, which represents the native species, both in terms of disulfides and conformation. The non-native disulfide intermediates such as MFI, I-1, I-4, I-5, and I-6 lie in the local energy minima, from where they have to be re-activated to reach the native state.

CONCLUSIONS

The oxidative folding of AAI clearly shows the interdependence of conformational folding and the assembly of native disulfide bonds. Because of its complexity, such a process needs to be analyzed both at the level of individual disulfide species and at the level of individual amino acid residues. The present work illustrates how biophysical techniques can be combined to achieve this end.

Because of the considerable local and global heterogeneity at the start of oxidative folding, the reduced protein cannot be actively driven or directed by the non-covalent interactions that stabilize the native three-dimensional structure. Rather, folding is directed by specific covalent interactions (*i.e.* disulfide bonds), which can be formed without notably restricting the extensively unfolded and mobile chain. The formation of non-native disulfide bonds can fulfil these requirements. The conversion from the non-native disulfide isomers is guided by non-covalent interactions stabilizing native secondary and tertiary structure. In this way, the disulfide bonds restrict the search in conformational space by cross-linking the protein in its unfolded state and thus decreasing its entropy.

Acknowledgments—We thank D. Craik, N. Daly, C. Guarnaccia, and J. A. Jones for help and useful discussions.

REFERENCES

1. Anfinsen, C. B. (1973) *Science* **181,** 223–230
2. Wedemeyer, W. J., Welker, E., Narayan, M., and Scheraga, H. A. (2000) *Biochemistry* **39,** 4207–4216
3. Creighton, T. (1974) *J. Mol. Biol.* **87,** 579–602
4. Weissman, J. S., and Kim, P. S. (1991) *Science* **253,** 1386–1393
5. Welker, E., Narayan, M., Wedemeyer, W. J., and Scheraga, H. A. (2001) *Proc. Natl. Acad. Sci. U. S. A.* **98,** 2312–2316
6. Scheraga, H. A., Wedemeyer, W. J., and Welker, E. (2001) *Methods Enzymol.* **341,** 189–221
7. Welker, E., Narayan, M., Volles, M. J., and Scheraga, H. A. (1999) *FEBS Lett.* **460,** 477–479
8. Narayan, M., Welker, E., Wedemeyer, W. J., and Scheraga, H. A. (2000) *Acc. Chem. Res.* **33,** 805–812
9. Chang, J. Y., Li, L., and Bulychev, A. (2000) *J. Biol. Chem.* **275,** 8287–8289
10. Chang, J. Y., Canals, F., Schindler, P., Querol, E., and Aviles, F. X. (1994) *J. Biol. Chem.* **269,** 22087–22094
11. Chang, J. Y. (1995) *J. Biol. Chem.* **270,** 25661–25666
12. Chang, J. Y., Schindler, P., and Chatrenet, B. (1995) *J. Biol. Chem.* **270,**

11992–11997
13. Chang, J. Y., and Li, L. (2000) *J. Protein Chem.* **21,** 203–213
14. Chang, J. Y., Li, L., Canals, F., and Aviles, F. X. (2000) *J. Biol. Chem.* **275,** 14205–14211
15. Chang, J. Y., Li, L., and Lai, P. H. (2001) *J. Biol. Chem.* **276,** 4845–4852
16. Chang, J. Y. (2002) *J. Biol. Chem.* **277,** 120–126
17. Chang, J. Y. (1999) *J. Biol. Chem.* **274,** 123–128
18. Chang, J. Y. (1996) *Biochemistry* **35,** 11702–11709
19. van den Berg, B., Chung, E. W., Robinson, C. V., and Dobson, C. M. (1999) *J. Mol. Biol.* **290,** 781–796
20. Heitz, A., Chiche, L., Le-Nguyen, D., and Castro, B. (1995) *Eur. J. Biochem.* **233,** 837–846
21. Daly, N. L., Clark, R. J., and Craik, D. J. (2003) *J. Biol. Chem.* **278,** 6314–6322
22. Milner, S. J., Carver, J. A., Ballard, F. J., and Francis, G. L. (1999) *Biotechnol. Bioeng.* **62,** 693–703
23. van den Berg, B., Chung, E. W., Robinson, C. V., Mateo, P. L., and Dobson, C. M. (1999) *EMBO J.* **18,** 4794–4803
24. Staley, J. P., and Kim, P. S. (1992) *Proc. Natl. Acad. Sci. U. S. A.* **89,** 1519–1523
25. Miller, J. A., Narhi, L. O., Hua, Q. X., Rosenfeld, R., Arakawa, T., Rohde, M., Prestrelski, S., Lauren, S., Stoney, K. S., Tsai, L., *et al.* (1993) *Biochemistry* **32,** 5203–5213
26. Shimotakahara, S., Rios, C. B., Laity, J. H., Zimmerman, D. E., Scheraga, H. A., and Montelione, G. T. (1997) *Biochemistry* **36,** 6915–6929
27. Laity, J. H., Lester, C. C., Shimotakahara, S., Zimmerman, D. E., Montelione, G. T., and Scheraga, H. A. (1997) *Biochemistry* **36,** 12683–12699
28. Biely, P., Mislovicova, D., Markovic, O., and Kalac, V. (1988) *Anal. Biochem.* **172,** 176–179
29. Pearson, M. A., Karplus, P. A., Dodge, R. W., Laity, J. H., and Scheraga, H. A. (1998) *Protein Sci.* **7,** 1255–1258
30. Escher, S. E., Sticht, H., Forssmann, W. G., Rosch, P., and Adermann, K. (1999) *J. Pept. Res.* **54,** 505–513
31. Hua, Q. X., Jia, W., Frank, B. H., Phillips, N. F., and Weiss, M. A. (2002) *Biochemistry* **41,** 14700–14715
32. Goransson, U., and Craik, D. J. (2003) *J. Biol. Chem.* **278,** 48188–48196
33. Cemazar, M., Zahariev, S., Lopez, J. J., Carugo, O., Jones, J. A., Hore, P. J., and Pongor, S. (2003) *Proc. Natl. Acad. Sci. U. S. A.* **100,** 5754–5759
34. Jarrett, N. M., Djavadi-Ohaniance, L., Willson, R. C., Tachibana, H., and Goldberg, M. E. (2002) *Protein Sci.* **11,** 2584–2595
35. Chen, H., Zhang, G., Zhang, Y., Dong, Y., and Yang, K. (2000) *Biochemistry* **39,** 12140–12148
36. Kubo, S., Chino, N., Kimura, T., and Sakakibara, S. (1996) *Biopolymers* **38,** 733–744
37. Tachibana, H., Ohta, K., Sawano, H., Koumoto, Y., and Segawa, S. (1994) *Biochemistry* **33,** 15008–15016
38. Chagolla-Lopez, A., Blanco-Labra, A., Patthy, A., Sanchez, R., and Pongor, S. (1994) *J. Biol. Chem.* **269,** 23675–23680
39. Lozanov, V., Guarnaccia, C., Patthy, A., Foti, S., and Pongor, S. (1997) *J. Pept. Res.* **50,** 65–72
40. Lu, S., Deng, P., Liu, X., Luo, J., Han, R., Gu, X., Liang, S., Wang, X., Li, F., Lozanov, V., Patthy, A., and Pongor, S. (1999) *J. Biol. Chem.* **274,** 20473–20478
41. Pereira, P. J., Lozanov, V., Patthy, A., Huber, R., Bode, W., Pongor, S., and Strobl, S. (1999) *Structure Fold. Des.* **7,** 1079–1088
42. Carugo, O., Lu, S., Luo, J., Gu, X., Liang, S., Strobl, S., and Pongor, S. (2001) *Protein Eng.* **14,** 639–646
43. Craik, D. J., Daly, N. L., and Waine, C. (2001) *Toxicon* **39,** 43–60
44. Han, Y., Albercio, F., and Barany, G. (1997) *J. Org. Chem.* **62,** 4307–4312
45. Soffe, N., Boyd, J., and Leonard, M. (1995) *J. Magn. Reson. A* **116,** 117–121
46. Scheffler, J. E., Cottrell, C. E., and Berliner, L. J. (1985) *J. Magn. Reson.* **63,** 199–201
47. Hore, P. J., and Broadhurst, R. W. (1993) *Prog. Nucl. Magn. Reson. Spectrosc.* **25,** 345–402
48. Maeda, K., Lyon, C. E., Lopez, J. J., Cemazar, M., Dobson, C. M., and Hore, P. J. (2000) *J. Biomol. NMR* **16,** 235–244
49. Peti, W., Smith, L. J., Redfield, C., and Schwalbe, H. (2001) *J. Biomol. NMR* **19,** 153–165
50. Klein-Seetharaman, J., Oikawa, M., Grimshaw, S. B., Wirmer, J., Duchardt, E., Ueda, T., Imoto, T., Smith, L. J., Dobson, C. M., and Schwalbe, H. (2002) *Science* **295,** 1719–1722
51. Redfield, C., Schulman, B. A., Milhollen, M. A., Kim, P. S., and Dobson, C. M. (1999) *Nat. Struct. Biol.* **6,** 948–952
52. Kauzmann, W. (1959) *Adv. Protein Chem.* **14,** 1–36
53. Gilbert, H. F. (1997) *J. Biol. Chem.* **272,** 29399–29402
54. Kainuma, K., Ookura, T., and Kawamura, Y. (1995) *J. Biochem.* (*Tokyo*) **117,** 208–215
55. Ciaffi, M., Paolacci, A. R., Dominici, L., Tanzarella, O. A., and Porceddu, E. (2001) *Gene* (*Amst.*) **265,** 147–156
56. Shimoni, Y., Zhu, X. Z., Levanony, H., Segal, G., and Galili, G. (1995) *Plant Physiol.* **108,** 327–335
57. Li, C. P., and Larkins, B. A. (1996) *Plant Mol. Biol.* **30,** 873–882
58. Takemoto, Y., Coughlan, S. J., Okita, T. W., Satoh, H., Ogawa, M., and Kumamaru, T. (2002) *Plant Physiol.* **128,** 1212–1222
59. McCarthy, A. A., Haebel, P. W., Torronen, A., Rybin, V., Baker, E. N., and Metcalf, P. (2000) *Nat. Struct. Biol.* **7,** 196–199
60. Schultz, C. P. (2000) *Nat. Struct. Biol.* **7,** 7–10